International Journal of advancement in electronics and computer engineering (IJAECE)
Volume 15, Issue 01, Jan. 2026, pp.121-127, ISSN 2278 -1412

DESIGN AND PERFORMANCE ANALYSIS OF A MULTIBAND METAMATERIAL-INSPIRED WEARABLE ANTENNA USING HEXAGONAL SPLIT-RING RESONATORS

Manish[1], Rajesh Kumar Rai [2], V. Thrimurthulu[3]

[1]*Research Scholar, Department of ECE Madhyanchal Professional University (MPU)* **,** *Department of ECE Bhopal,* msliet@gmail.com, *India*

[2]*Supervisor, Department of ECE Madhyanchal Professional University (MPU),* raj.rai1008@gmail.com, *India*

[3]*Co-Supervisor, Department of ECE , Associate Professor, MLRIT, Hyderabad, Telangana* vtmurthy.v@gmail.com, *India*

Abstract – The aim of this research was to develop a conformal, compact antenna operating at the 61.25 GHz band specifically for ingestible telemetry operations. The antenna was encapsulated within a biocompatible silicon capsule, limited to dimensions of 23 mm height by 9 mm diameter, to ensure the comfort of swallowing and reliability for implantable devices. The technique employed a simple and symmetrical antenna structure to assure consistent radiation characteristics within the complex environment of the gastrointestinal tract. To effectively moderate the high Specific Absorption Rate (SAR) and minimize tissue heating, the antenna was powered by 1W of energy, provided only in short burst modes with long intervals. This power control management plan was decisive for limiting the thermal effects. The outcomes from the investigation were highly optimistic. The designed antenna successfully maintained its intended bandwidth and showed predominantly good gain, verifying its robustness in the ingestible environment. Moreover, the efficiency of the antenna was established to be more than 50%. The study concluded that the antenna shows great potential to radiate effectively after the designed capsule antenna is swallowed, making it a viable solution for progressive ingestible sensing and communication. Biocompatibility and safety analysis and encapsulation was the main concern for the implantable design. Implantable designs are encapsulated in thin layers of biocompatible materials like to prevent direct contact between the radiating element and body gastrointestinal tract. Rigorous SAR evaluations were conducted using phantom based human models to ensure compliance with international safety standards (IEEE and ICNIRP). Furthermore, this research introduces a link budget analysis for biotelemetry communication.

Keywords: Multiband Antenna, Meta material-Inspired Antenna, Wearable Antenna, HSRR, SRR

1. INTRODUCTION

With recent advancements in the field of communication technology, antennas are being designed for application in wearable devices. The major requirements of an antenna to be suitable for use in a wearable device are compactness, compatibility, multiband operations, and a low specific absorption rate (SAR). In this context, a multiband antenna would be the preferred antenna because it involves a single antenna capable of trans-receiving more than one operating band, which is extremely suitable for a wearable device, where the scope of integrating multiple antennas for different frequencies is very low. Furthermore, its low SAR value ensures the safe use of antennas positioned near the human body. Therefore, several researchers have proposed innovative antenna designs, such as circular and hexagonal split- ring resonators (SRRs), rectangular SRRs, complementary SRRs (CSRRs), meander lines, extended radiator structures, and even reconfigurable structures that generate multiple bands through the application of switching circuits. Some of these antenna designs involve a meander-line structure accomplished on a perforated inset step ground plane for triple-band operation , an extended radiator structure on partially perforated ground plane for multiple-band operation , a PIN diode used to connect two slots of a coplanar waveguide (CPW) antenna for switching between multiple- band operations , a CSRR within a CPW antenna with the ground plane located at the periphery of the substrate for triple-band operation , and multiple hexagonal CSRRs on a hexagonal radiating surface in a CPW antenna for triple-band operation. Furthermore, a number of designs for CPW antennas have been accomplished, involving a combination of triangular SRRs and circular CSRRs on a flexible substrate for dual-band operation , a simple SRR-shaped radiator with ground on the same plane to generate dual bands a co-axial feed with a meandered L-shaped probe on a

simple rectangular patch to design a triple-band antenna a left-adjusted inset feed in a rectangular patch with CSRR on a defected ground structure to attain four bands [200], a circular patch with partial ground plane and parasitic T- and L-shaped stubs for achieving four bands , and a pentagon-shaped radiating patch edged with a circular slot and a parasitic E-shaped radiating element with partial ground plane for acquiring three bands In this work, a four-band antenna consisting of dual SRR and CSRR is presented for use in ISM (2.4 and 5.8 GHz), maritime radio navigation, aeronautical radio navigation, and Wi-Fi WLAN applications. The antenna is compact, and is verified for biomedical wearable applications using a four-layer human phantom model. The following points highlight the novelty of the proposed design: A single antenna is able to realize four different bands, thus allowing for ISM (2.4 GHz and 5.88 GHz), radio location, maritime radio location, aeronautical engineering, and Wi- Fi/WLAN applications. The two notch bands serve to efficiently eliminate the highly occupied extended UMTS and the bands pertaining to fixed mobile applications. Inexpensive and readily accessible FR4 material is used in the antenna's design. The antenna radiates at both the 2.4 GHz and 5.8 GHz biomedical bands, making it highly suitable for wearable applications with a very low SAR.The novelty of the proposed antenna also lies in its being a single monopole antenna that can operate at both the sub-6 GHz ISM bands (2.4 GHz and 5.8 GHz). Notably, the term meta material-inspired is used in this study because meta material properties are utilized to reduce patch size. In theory, the patch size for the 2.4 GHz band is usually a length of 38.03 mm and a breadth of 29.442 mm (area 1,119 mm2). When using meta materials, the patch dimensions can be reduced to a length of 24.63 mm and a breadth of 22 mm (area 541.86 mm2), indicating a 51.58% reduction in patch size.

2. DESIGN DIMENSIONS AND EVOLUTION OF THE ANTENNA

Fig. 1(a) illustrates the structural layout of the hexa-ring SRR multiband antenna, while Fig. 1(b) presents the completed prototype (fabricated). The antenna was constructed on a fire- resistant, 1.6 mm-thick glass epoxy foundation with a εr of 4.4. The overall dimensions were 35 mm (height) and 35 mm (width). The design of the proposed antenna features a hexagonal outer-ring-type structure along with a step feed to generate four bands covering 2.37–2.48 GHz, 2.8–3.2 GHz, 4.25–4.4 GHz, and 5.38–6.22 GHz, resonating at 2.43 GHz, 2.94 GHz, 4.35 GHz, and 5.75 GHz for the 2.4 GHz ISM band, radio location applications, aeronautical and radio navigation applications, and the 5.8 GHz ISM band, respectively. Furthermore, two hexagon- shaped SRRs were employed to generate band notches at 2.59 GHZ and 4.56 GHz, thereby eliminating interference from mobile communication networks.

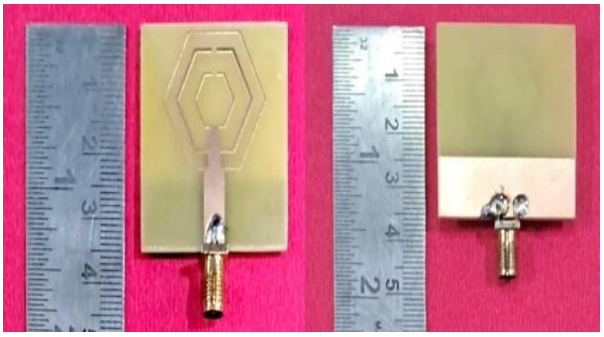

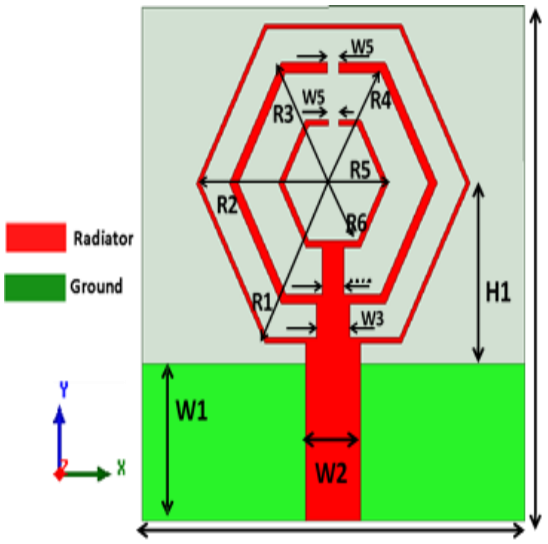

Fig. 1. (a) Dimensions and statistics of the proposed antenna; (b) Prototype (fabricated).

The evolution of the proposed antenna involved four consecutive steps, where the |S11| progressively improved with each step. As shown in Fig. 2(a), a hexagonal structure is utilized as the radiator in Step 1, with a dual band observed at 2.8–3.2 GHz and 5.0–6.6 GHz. In Step 2, a hexagonal ring-type structure is etched out from the radiator to form a hexagonal ring with a thickness of 0.37 mm (R1–R2), thereby increasing the electric length of the antenna, which then radiates at a lower frequency range of 2.2–2.4 GHz and 7.4–8.0 GHz. In Step 3, a hexagonal SRR is added to the structure using a step feed, which is responsible for generating a triple band at frequency ranges of 2.6–2.8 GHz, 4.1–4.5 GHz, and 5.2–5.7 GHz, while a notch band is formed at 4.55 GHz due to the generation of the CSRR structure. Finally, a hexagonal structure with a step feed is introduced, which improves the electric length of the structure and successfully achieves the four desired bands: 2.37–2.48 GHz, 2.8–3.2 GHz, 4.25–4.40 GHz, and 5.38–6.22 GHz. The reflection coefficient at each step is depicted in Fig. 2(b).

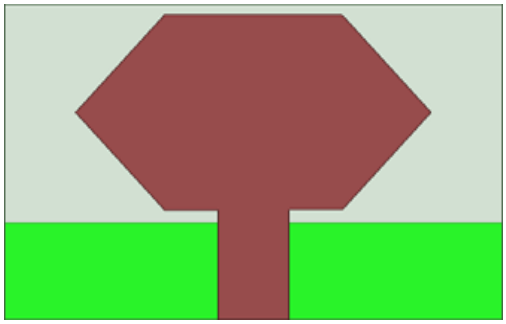

Step1

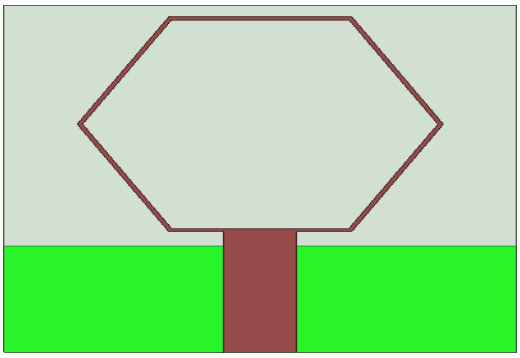

Step 2

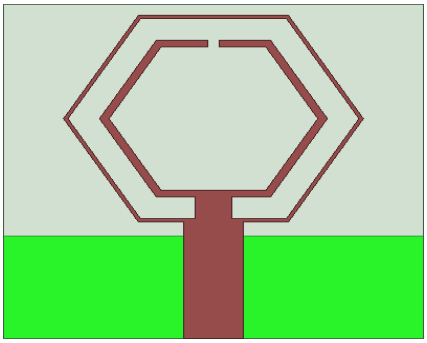

Step3

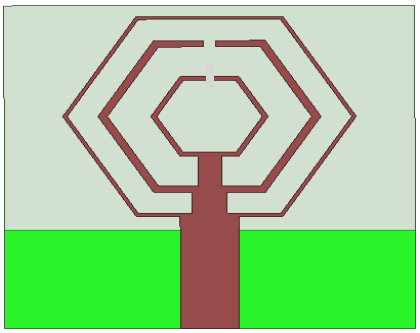

Step 4

Fig. 2. (a) Steps for designing the prototype antenna;

(b) Reflection coefficient of the development steps

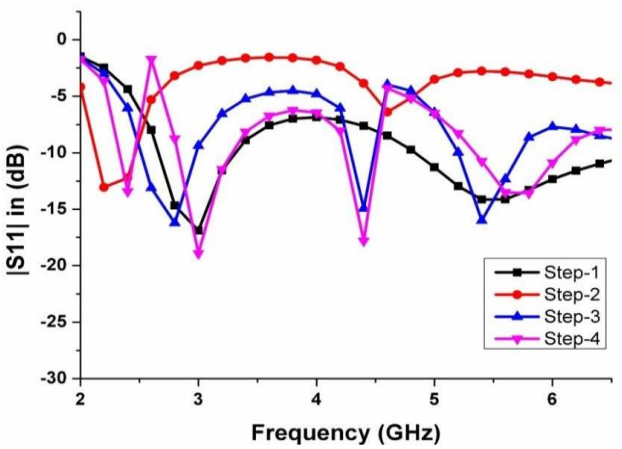

II. NOTCH ANALYSIS

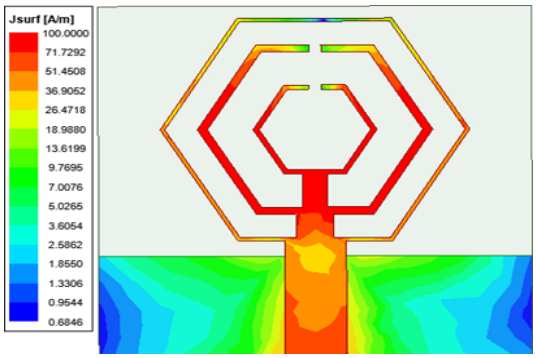

Fig;(a)

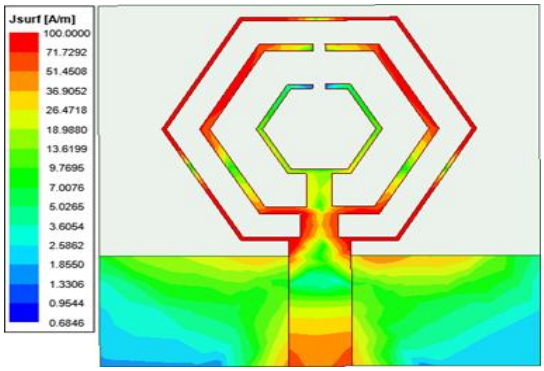

Fig;(b)

Fig. 3. (a) Surface current analysis of J_{surf} notch at 2.59 GHz (b) Surface current analysis of J_{surf} notch at 4.55 GHz.

2.1 Wearable Analysis

Among the four bands exhibited by the proposed antenna, 2.4 GHz and 5.8 GHz can be allocated for wearable and biomedical applications. Notably, since the antenna has a compact structure, it is considered highly desirable for use in wearable devices, To investigate this, a phantom model imitating the human wrist was employed, as depicted in Fig. 4.4. The thicknesses of the skin tissue, fat tissue, muscular tissue, and bone in the model were 2 mm, 5 mm, 30 mm, and 10 mm, respectively

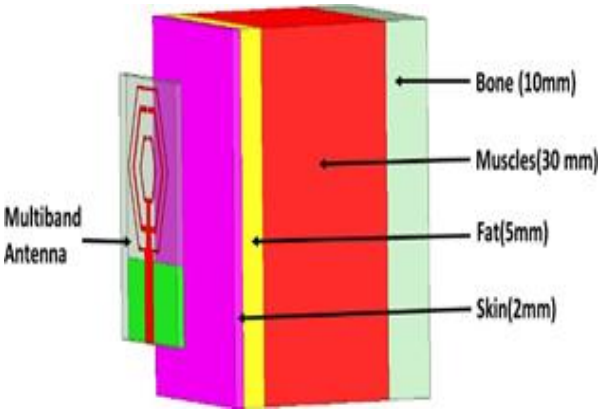

Fig. 4. The antenna and the phantom model

Table I. Characteristics of tissues at different operating frequencies

Operating frequency (GHz)	Tissue type	Relative Permittivity (ϵ_r)	Conductivity (S/m)	Loss tangent (σ)
2.4	Skin	38	1.464	0.283
	Fat	5.280	0.1045	0.145
	Muscle	52.729	1.7388	0.24194
	Bone	11.381	0.39431	0.2542
2.9	Skin	37.545	1.6875	0.27859
	Fat	5.234	0.12519	0.14826
	Muscle	52.18	2.0645	0.24524
	Bone	11.122	0.48526	0.27044
4.3	Skin	36.342	2.5443	0.29266
	Fat	5.0958	0.20011	0.16416
	Muscle	50.441	3.3093	0.27426
	Bone	10.38	0.79695	0.32097
5.8	Skin	35.114	3.717	0.32807
	Fat	4.9549	0.29313	0.18335
	Muscle	48.485	4.9615	0.31715
	Bone	9.6744	1.1544	0.36981

Since the human body is a lossy environment, placing an antenna too close to it results in significant radiation losses. Additionally, changes in operating frequency may alter the properties of tissues. The characteristics of different tissues with regard to operating frequency are presented in Table 4.3. In this study, the tissues were characterized according to the values depicted in the table 4.3 and their radiation values, such as |S11|. Radiation efficiency and the peak realized gain were analyzed by positioning the designed antenna 5 mm, 10 mm, 15 mm, and 20 mm from the phantom model. The results for |S11|, peak realized gain, and radiation efficiency are presented in Fig. 4.5(a), 4.5(b), and 4.5(c), respectively. A minor variation in |S11| is observed when the antenna is placed at a distance of 5 mm from the human body. Furthermore, Fig. 4.5(b) shows that the gain is substantial at lower frequencies at distances of 10 mm and 15 mm, while it is higher at higher frequencies. This observation can be attributed to the effect of grating lobe reflections from the skin at higher frequencies, which serve to enhance the gain . Therefore, these two positional distances were considered optimum for the placement of the antenna. The radiation efficiencies at 10 mm and 15 mm were found to range from 40% to 60% and from 60% to 80%, respectively, as shown in Fig. 4.5(c).

The SAR assesses the rate at which energy is absorbed by the body upon exposure to an RF electromagnetic field in biological systems and tissue models. To be safely used on the human body for wearable applications, the antenna's SAR must not exceed 1.6 W/kg. The SAR values measured on 10 g of sample tissue with 0.5 W of input power at frequencies of 2.4 GHz, 2.9 GHz, 4.3 GHz, and 5.8 GHz were 0.3661, 0.4998, 0.1968, and 0.1683 W/kg, as shown in Fig. 4.6(a), 4.6(b), 4.6(c), and 4.6(d), respectively. Since the measured SAR values were less than the prescribed values, the antenna was considered safe for use in a wearable.

III. RESULTS AND DISCUSSION

A compact, metamaterial-based, structured quad-band antenna intended for WLAN, ISM band (2.4 GHz and 5.8 GHz), and aeronautical and radio navigation applications is proposed in this study. The antenna exhibited sharp reflection coefficients for the first three bands and a wider bandwidth for the fourth band. Furthermore, the bands were restricted by the application of SRR, using which notches were deliberately created at 2.59 GHZ and 4.56 GHz to eliminate interference by mobile communication, as depicted in Fig. 4.7(a).

The results show that the proposed antenna achieved a considerably high gain - averaging at 3 GHz, with the peak gain reaching 4.5 GHz - indicating that it is effective for near-field communications. Furthermore, as shown in Fig. 4.7(b), the gain is disrupted and negative at 2.59 GHZ and 4.56 GHz, which represent the notch bands. Moreover, the measured results closely resembled the simulated results, with slight discrepancies between the simulated and measured waveform readings caused primarily by measurement and fabrication errors. The radiation efficiency remained stable, averaging at around 90%, except at the notch bands, where it reduced to 15% and 40%, as illustrated in Fig. 4.7(c).

The plots for radiation efficiency and gain verified the presence of notch bands. Notably, the antenna was evaluated using a vector network analyzer (VNA) in an anechoic room. Fig. 4.7(d) displays the radiation patterns (normalized, simulated, and measured) obtained at 2.4 GHz, 2.9 GHz, 4.3 GHz, and 5.8 GHz, while the S-parameters measured using the VNA are illustrated in Fig. 4.7(e).

The stability of the antenna was verified by closely examining the radiation pattern, the outcomes of which confirmed the antenna's radiation properties. Table 4.4 presents an analytical comparison of the proposed antenna and those reported in recently published studies

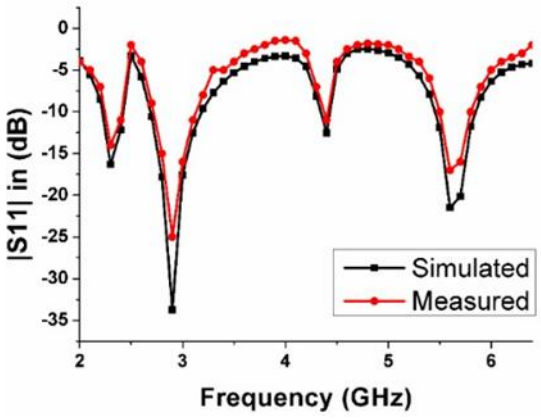

Fig(a)

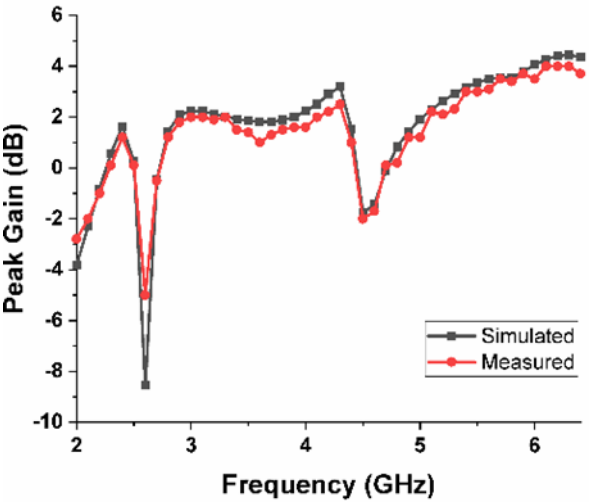

Fig(b)

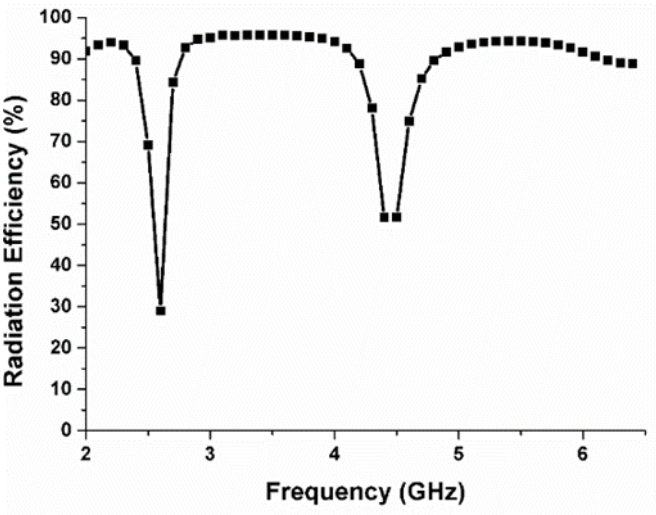

Fig(C)

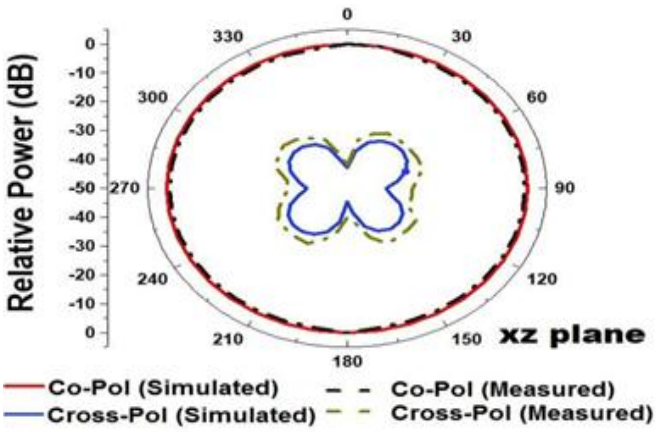

Antenna pattern at 2.4 GHz (E-plane)

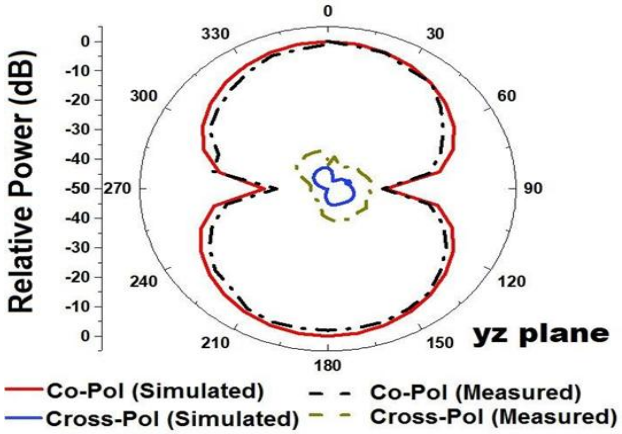

Antenna pattern at 2.4 GHz (H-plane)

IV. CONCLUSION

A quad-band antenna is integral to WLAN, ISM band (2.4 GHz and 5.8 GHz), and aeronautical and radio navigation applications. In this regard, the antenna proposed in this study is found to be suitable for wearable applications because it allows transmission at both the biomedical application bands of 2.4 GHz and 5.8 GHz. Its suitability for WLAN, radio- location, and navigation applications is an added advantage. Furthermore, notch bands at 2.59 GHz and 4.56 GHz help to accurately reject the mobile communication band. In addition, owing to its metamaterial inspired structure, an overall reduction of 51.58% was achieved for the patch size of the antenna. Overall, the proposed antenna is highly suitable for multiple- band operation in wearable applications.

REFERENCES

[1]. S. Ahmad, A. Ghaffar, N. Hussain, and N. Kim, “Compact dual-band antenna with paired l-shape slots for on-and off-body wireless communication,” Sensors, vol. 21, no. 23, 2021, doi: 10.3390/s21237953.

[2]. C. Zhao and W. Geyi, “Design of a dual band dual mode antenna for on/off body communications,” Microw. Opt. Technol. Lett., vol. 62, no. 1, pp. 514–520, 2020, doi: 10.1002/mop.32085.

[3]. M. Mustaqim, B. A. Khawaja, H. T. Chattha, K. Shafique, M. J. Zafar, and M. Jamil, “Ultra-wideband antenna for wearable Internet of Things devices and wireless body area network applications,” Int. J. Numer. Model. Electron. Networks, Devices Fields, vol. 32, no. 6, pp. 1–12, 2019, doi: 10.1002/jnm.2590.

[4]. S. M. Hosseini Varkiani and M. Afsahi, “Grounded CPW multi-band wearable antenna for MBAN and WLAN applications,” Microw. Opt. Technol. Lett., vol. 60, no. 3, pp. 561–568, 2018, doi: 10.1002/mop.31012.

[5]. F. Khajeh-Khalili and Y. Khosravi, “A novel wearable wideband antenna for application in wireless medical communication systems with jeans substrate,” J. Text. Inst., vol. 112, no. 8, pp. 1266–1272, 2021, doi: 10.1080/00405000.2020.1809909.

[6]. D. Mitra et al., “Conductive electrifi and nonconductive ninjaflex filaments based flexible microstrip antenna for changing conformal surface applications,” Electron., vol. 10, no. 7, 2021, doi: 10.3390/electronics10070821.

[7]. C. Wang, L. Zhang, and X. Wu, “A wearable flexible microstrip antenna based on the floating-ground backplane,” International Journal of RF and Microwave Computer-Aided Engineering, vol. 31, no. 1. 2021. doi: 10.1002/mmce.22481.

[8]. G. Santhakumar, R. Vadivelu, A. Perumal and D. Selvaraj, “A flexible microstrip antenna for health monitoring application in wireless body area network,” Int. J. Sci. Technol. Res., vol. 9, no. 3, pp. 7088–7092, 2020.

[9]. J. Zhu et al., “Strain-Insensitive Hierarchically Structured Stretchable Microstrip Antennas for Robust Wireless Communication,” Nano-Micro Lett., vol. 13, no. 1,pp. 1–12, 2021, doi: 10.1007/s40820-021-00631-5.

[10]. .H. Hamad and A. Mian, “Radio frequency response of flexible microstrip patch antennas under compressive and bending loads using multiphysics modeling approach,” Int. J. RF Microw. Comput. Eng., vol. 29, no. 3, pp. 1–11, 2019, doi: 10.1002/mmce.21649.

[11]. W. A. Awan, N. Hussain, and T. T. Le, “Ultra-thin flexible fractal antenna for2.45 GHz application with wideband harmonic rejection,” AEU - Int. J. Electron. Commun., vol. 110, p. 152851, 2019, doi: 10.1016/j.aeue.2019.152851.

[12]. E. Thangaselvi and K. Meena alias Jeyanthi, “Implementation of flexible denim nickel copper rip stop textile antenna for medical application,” Cluster Comput., vol. 22, no. s1, pp. 635–645, 2019, doi: 10.1007/s10586-017-1647-0

[13]. H. K. Bhaldar et al., “Design of Circular Microstrip Textile Antenna for UWB Application,” IETE J. Res., 2021, doi:

10.1080/03772063.2021.1982416.

[14]. L. Berkelmann and D. Manteuffel, "Characterization of Wearable and Implanted Antennas: Test Procedure and Range Design," *IEEE Trans. Antennas Propag.*, vol. 70, no. 4, pp. 2593–2601, 2022, doi: 10.1109/TAP.2021.3126386.

[15]. D. Andre and D. L. Wolf, "Recent advances in free-living physical activity monitoring: A review," *J. Diabetes Sci. Technol.*, vol. 1, no. 5, pp. 760–767, 2007, doi: 10.1177/193229680700100522.